Electronic supplementary information

Wool graft polyacrylamidoxime as the adsorbent for adsorption both cationic and anionic toxic ions from aqueous solutions

Chun Cao,[a,b] Hongliang Kang,*[a] Ning Che,[a,b] Zhijing Liu,[a,b] Pingping Li,[a,b] Chao Zhang,[a,b] Weiwei Li,[a,b] Ruigang Liu*[a] and Yong Huang*[ac]

[a] *Sate Key Laboratory of Polymer Physics and Chemistry, Beijing National Laboratory of Molecular Sciences, Institute of Chemistry, Chinese Academy of Sciences, Beijing 100190, China*

[b] *University of Chinese Academy of Science, Beijing, 100049, China*

* Corresponding authors. Tel./fax: +86-10-8268573. E-mail: rgliu@iccas.acn.

Table S1. The exploration of the reaction conditions of first step

No.	AN (mL)	Initiator ($\times 10^5$ mol/L)	Solvent (mL)		$T/°C$	$G_d{}^a$
			Urea (8 M)	DMAC		
1	2.0	2.49	15	0	65	12.98%
2	2.0	3.74	15	0	65	34.52%
3	2.0	5.0	15	0	65	55.25%
4	2.0	9.96	15	0	65	42.48%
5	2.0	19.9	15	0	65	22.40%
6	0.5	5.0	15	0	65	5.68%
7	1.0	5.0	15	0	65	14.34%
8	1.5	5.0	15	0	65	38.46%
9	2.0	5.0	15	0	65	55.25%
10	2.5	5.0	15	0	65	55.89%
11	3.0	5.0	15	0	65	56.17%
12	3.5	5.0	15	0	65	54.82%
13	2.0	5.0	15	0	45	0
14	2.0	5.0	15	0	50	4.50%
15	2.0	5.0	15	0	55	4.61%
16	2.0	5.0	15	0	60	12.18%
17	2.0	5.0	15	0	65	55.25%
18	2.0	5.0	15	0	70	53.42%
19	2.0	5.0	12	3	65	0.17%
20	2.0	5.0	10	5	65	0.08%
21	2.0	5.0	7.5	7.5	65	0.05%
22	2.0	5.0	5	10	65	0
23	2.0	5.0	0	15	65	0

^{a} G_d was calculated by using Eq. 1, 0.25 g wool was added in each experiment.
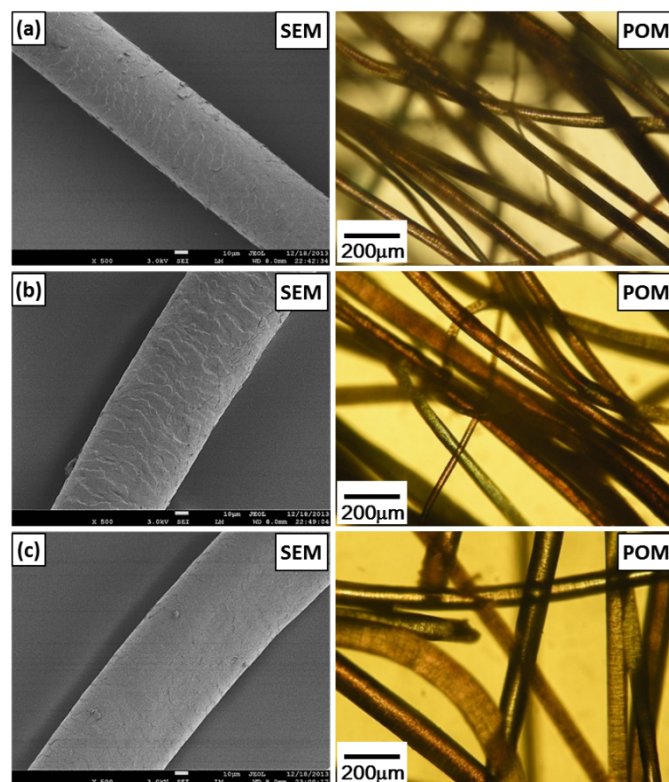
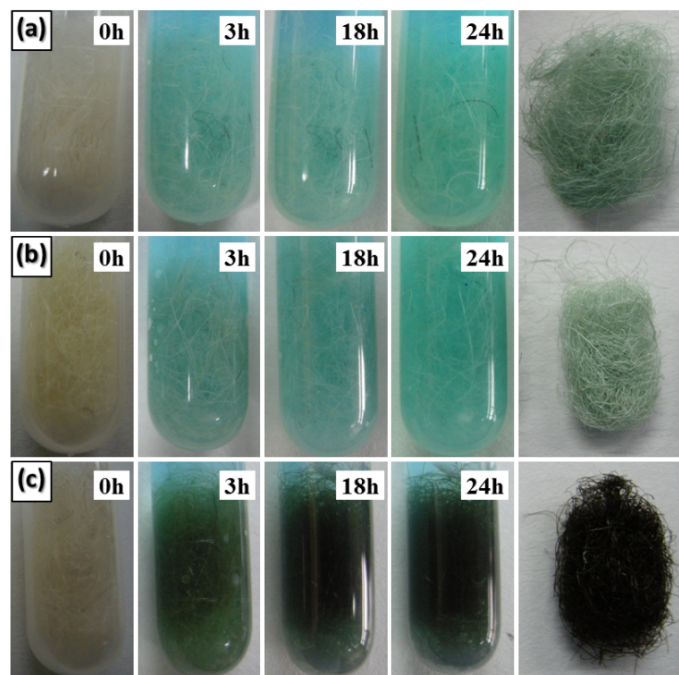**Fig. S1.** The typical SEM (left) and POM (right) images of (a) wool, (b) W-*g*-PAN, and (c) W-*g*-PAO.

Fig. S2. Photos of the (a) wool, (b) W-*g*-PAN, and (c) W-*g*-PAO samples that immersed in the CuSO$_4$ solutions at the time noted in the photos. The last column is the dried samples after immersed in CuSO$_4$ solutions for 24 h.
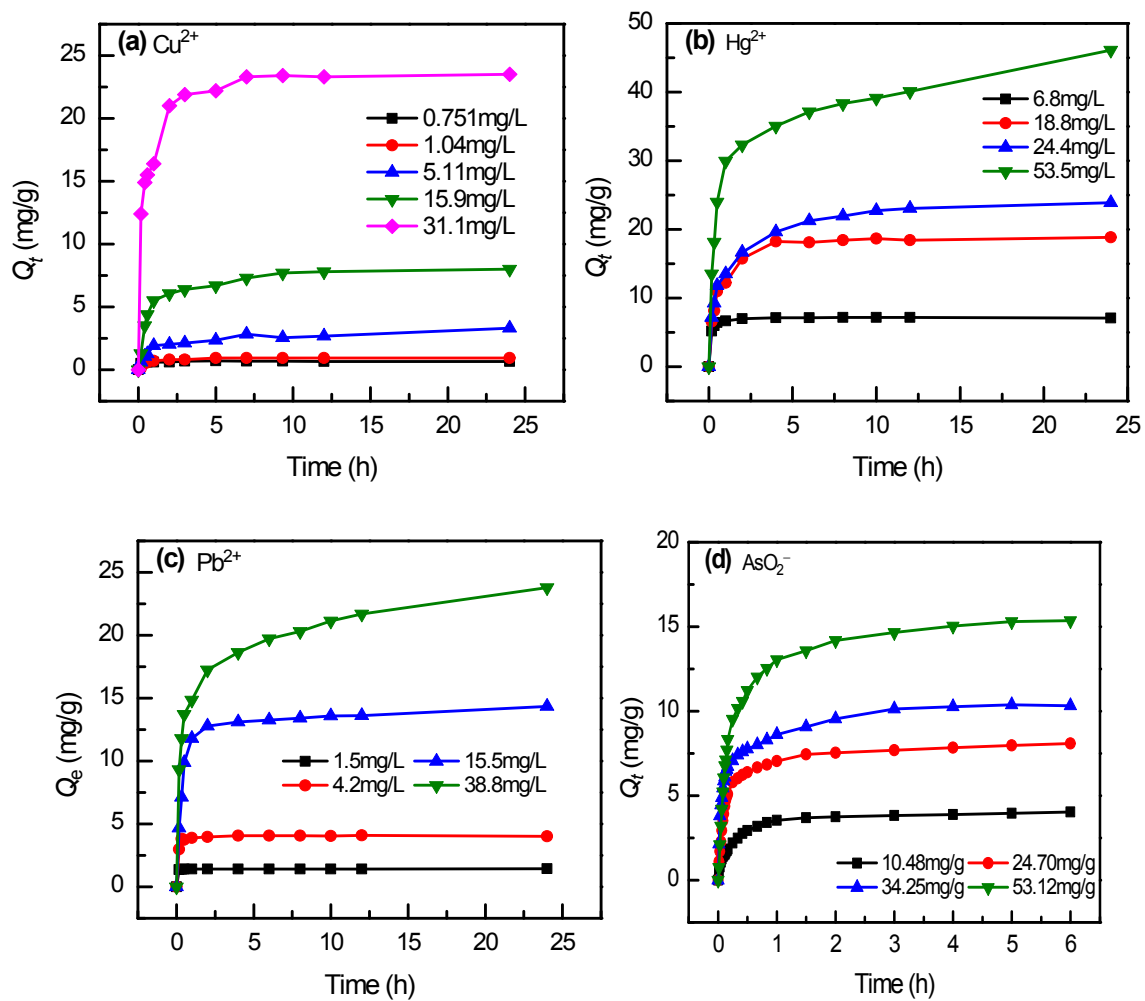
Fig. S3. The adsorption kinetics of (a) Cu^{2+}, (b) Hg^{2+}, (c) Pd^{2+}, and (d) AsO_2^- ions from water at different initial concentration.
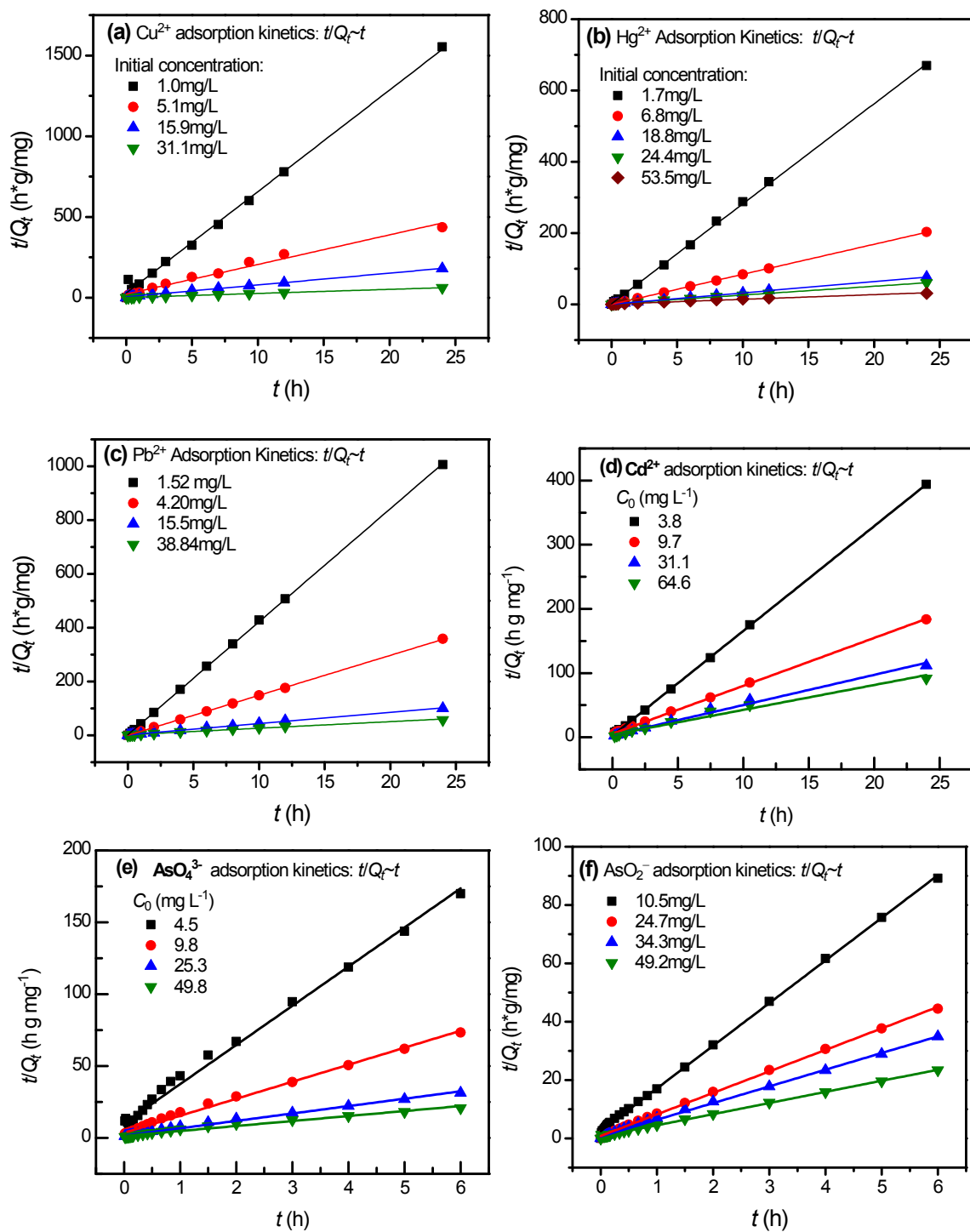
Fig. S4. Quasi-two adsorption kinetic curve of (a) Cu^{2+}, (b) Hg^{2+}, (c) Pd^{2+}, (d) Cd^{2+}, (e) AsO_4^{3-} and (f) AsO_2^{-}. The lines are the fitting results by using Eq. 3.

Table S3. The correlation coefficient R^2 by using the linear fitting of pseudo-second order models

Pb^{2+}		Hg^{2+}		Cd^{2+}		AsO_4^{3-}		AsO_2^{-}	
C_0 (mg g^{-1})	R^2	C_0 (mg g^{-1})	R^2	C_0 (mg g^{-1})	R^2	C_0 (mg g^{-1})	R^2	C_0 (mg g^{-1})	R^2
1.52	0.999	6.83	0.999	3.76	0.999	4.52	0.993	10.48	0.999
4.20	0.999	18.8	0.999	9.70	0.999	9.75	0.995	24.70	0.999
15.50	0.999	24.36	0.998	31.1	0.991	25.3	0.992	34.25	0.999
38.84	0.991	53.54	0.991	64.6	0.981	49.82	0.982	53.12	0.996

The non-linear pseudo-first order model and the non-linear pseudo-second order model are described in eqs. S1 and 3, respectively.

$$Q_t = Q_e\left(1 - e^{-kt}\right) \qquad\qquad (S1)$$

where t is the contact time of adsorption procedure, Q_t and Q_e are the adsorbed toxic ions on the adsorbent at adsorption time t and at equilibrium state, which were calculated by using eqs. S1 and 3. k are the adsorption rate constant of the non-linear pseudo-first order model respectively.
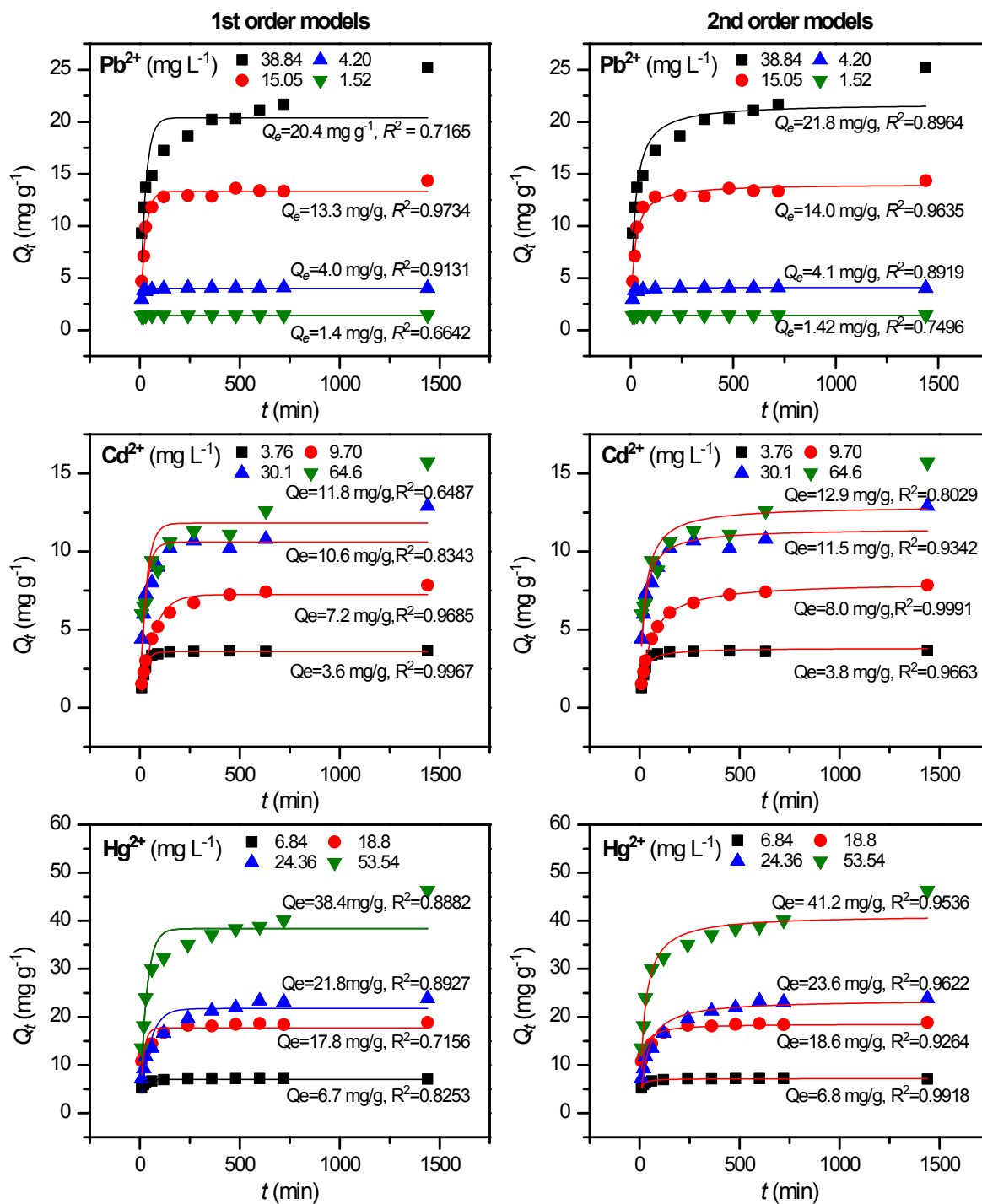
Fig. S5. The non-linear fitting of pseudo-first order (left) and pseudo-second (right) order models for Pb^{2+}, Cd^{2+}, and Hg^{2+} cations.
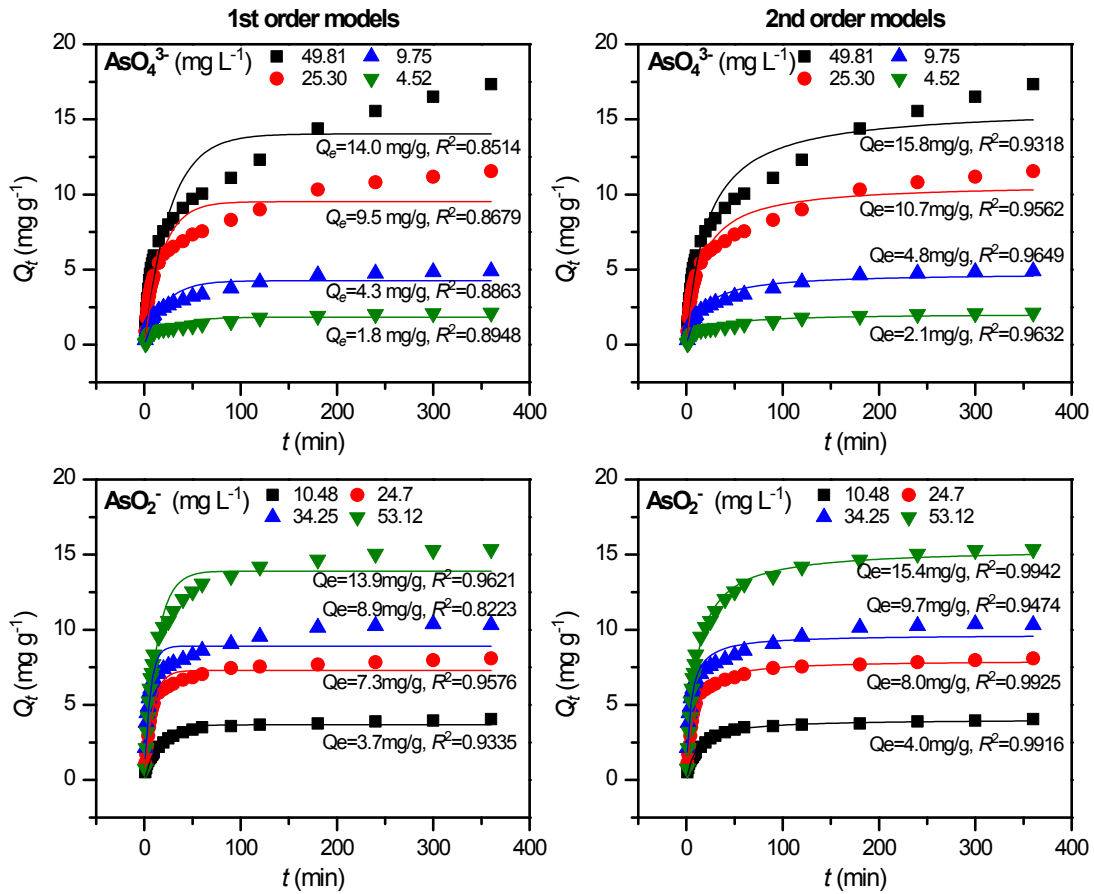
Fig. S6. The non-linear fitting of pseudo-first order (left) and pseudo-second (right) order models for AsO_4^{3-} and AsO_2^- anions.

Table S4. The correlation coefficient R^2 by using the non-linear fitting of pseudo-second order models

Pb^{2+}		Hg^{2+}		Cd^{2+}		AsO_4^{3-}		AsO_2^-	
C_0 (mg g^{-1})	R^2	C_0 (mg g^{-1})	R^2	C_0 (mg g^{-1})	R^2	C_0 (mg g^{-1})	R^2	C_0 (mg g^{-1})	R^2
1.52	0.750	6.83	0.992	3.76	0.966	4.52	0.963	10.48	0.992
4.20	0.892	18.8	0.926	9.70	0.999	9.75	0.965	24.70	0.993
15.50	0.964	24.36	0.962	31.1	0.934	25.3	0.956	34.25	0.947
38.84	0.896	53.54	0.954	64.6	0.803	49.82	0.932	53.12	0.994

Table S5. The correlation coefficient R^2 by using the non-linear fitting of pseudo-first order models

Pb^{2+}		Hg^{2+}		Cd^{2+}		AsO_4^{3-}		AsO_2^-	
C_0 (mg g^{-1})	R^2	C_0 (mg g^{-1})	R^2	C_0 (mg g^{-1})	R^2	C_0 (mg g^{-1})	R^2	C_0 (mg g^{-1})	R^2
1.52	0.664	6.83	0.888	3.76	0.997	4.52	0.895	10.48	0.934
4.20	0.913	18.8	0.893	9.70	0.969	9.75	0.886	24.70	0.958
15.50	0.973	24.36	0.716	31.1	0.834	25.3	0.868	34.25	0.822
38.84	0.716	53.54	0.825	64.6	0.649	49.82	0.851	53.12	0.962

The Freundlich model and Temkin model are described in eqs. S1 and S2, respectively.

$$lgQ_e = lgK_F + \frac{1}{n}lgC_e \qquad\qquad (S2)$$

$$Q_e = \frac{RT}{b}ln(aC_e) \qquad\qquad (S3)$$

where C_e(mg L^{-1}) is the concentration of the toxic ions at equilibrium state in the solution, Q_e is the adsorbed toxic ions on the adsorbent at equilibrium stateK_L and K_F are the adsorption equilibrium constant in Langmiur and Freundlich model, respectively. n is the characteristic constant relative to adsorption strength, R is gas constant, a and b are Temkin adsorption constants, and T is temperature.
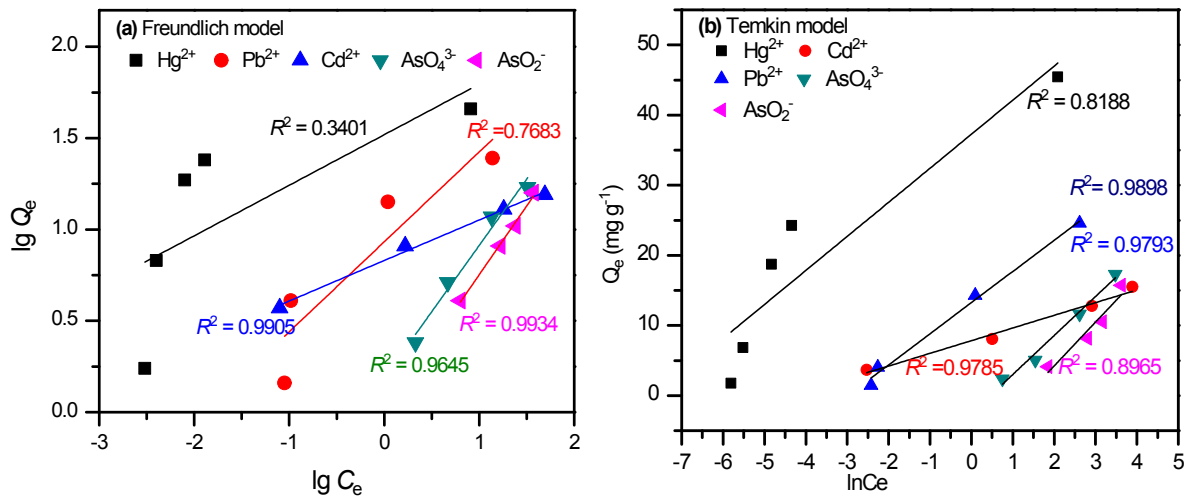

Fig. S7. The adsorption isotherms fitted by (a) Freundlich and (b) Temkin model, several data points of Hg^{2+} and Pb^{2+} are considerably close to each other due to the strong adsorption capacity of Hg^{2+}, Pb^{2+} on adsorbent W-g-PAO.

Table S6. The correlation coefficient R^2 of different adsorption isotherm models for Cd^{2+}, Pb^{2+}, Hg^{2+}, AsO_4^{3-} and AsO_2^-.

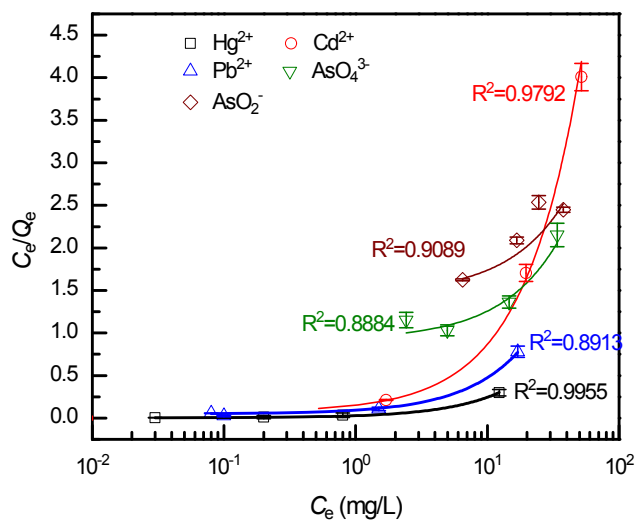|	Cd^{2+}	Pb^{2+}	Hg^{2+}	AsO_4^{3-}	AsO_2^-
Freundlich model	0.9905	0.7683	0.3401	0.9645	0.9934
Langmuir model	0.9913	0.9945	0.9999	0.9872	0.8386
Temkin model	0.9785	0.9898	0.8188	0.9793	0.8965

Fig. S8. Semi-log plot of Fig. 4b.